tre-Assistant affecté au CNRS (E.R.A. No. 82) Laboratoire des Hétérocycles du phosphore et de l'azote, Université Paul Sabatier, Toulouse, France. Visiting Professor at the University of Massachusetts, 1975–1976.
(3) (a) R. R. Holmes, *J. Am. Chem. Soc.*, **97**, 5379 (1975); (b) *ibid.*, **96**, 4143 (1974).
(4) (a) H. Wunderlich and D. Mootz, *Acta Crystallogr. Sect. B*, **30**, 935 (1974); (b) H. Wunderlich, *ibid.*, **30**, 939 (1974); (c) H. Wunderlich, personal communication.
(5) W. S. Sheldrick, personal communication.
(6) R. K. Brown and R. R. Holmes, *J. Am. Chem. Soc.*, **99**, 3326 (1977).
(7) R. Sarma, F. Ramirez, and J. F. Maracek, *J. Org. Chem.*, **41**, 473 (1976).
(8) M. Eisenhut, R. Schmutzler, and W. S. Sheldrick, *J. Chem. Soc., Chem. Commun.*, 144 (1973), and personal communication.
(9) R. R. Holmes, *Acc. Chem. Res.*, **5**, 296 (1972), and references cited therein.
(10) (a) R. R. Holmes and J. A. Deiters, *J. Am. Chem. Soc.*, **99**, 3318 (1977); (b) J. A. Deiters, J. C. Gallucci, T. E. Clark, and R. R. Holmes, *J. Am. Chem. Soc.*, **99**, 5461 (1977).
(11) R. S. Berry, *J. Chem. Phys.*, **32**, 933 (1960).
(12) M. G. Newton, J. E. Collier, and R. Wolf, *J. Am. Chem. Soc.*, **96**, 6888 (1974).
(13) P. F. Meunier, J. A. Deiters, and R. R. Holmes, *Inorg. Chem.*, **15**, 2572 (1976).
(14) R. Burgada, *Ann. Chim. (Paris)*, [13] **8**, 347 (1963).
(15) (a) W. R. Busing and H. A. Levy, *J. Chem. Phys.*, **26**, 563 (1957); (b) R. C. G. Killean, D. F. Grant, and J. L. Lawrence, *Acta Crystallogr., Sect. B*, **25**, 374 (1969).
(16) "International Tables for X-ray Crystallography", Vol. I, Kynoch Press, Birmingham, England, 1969, p 101.
(17) The function minimized was $\sum w(|F_o| - |F_c|)^2$.
(18) D. T. Cromer and J. T. Waber, *Acta Crystallogr.*, **18**, 104 (1965).
(19) R. F. Stewart, E. R. Davidson, and W. T. Simpson, *J. Chem. Phys.*, **42**, 3175 (1965).
(20) C. K. Johnson's program ORTEP, Report ORNL-3794, Oak Ridge National Laboratory, Oak Ridge, Tenn., 1965.
(21) M. Sanchez, Thesis No. 433, Paul Sabatier University, Toulouse, France.
(22) N. Tikhonina, V. Gilyarov, and M. Kabachnik, *Izv. Akad. Nauk SSSR, Ser. Khim.*, No. 6, 1426 (1973).
(23) Reference 16, p 99.
(24) G. Germain, P. Main, and M. M. Woolfson, *Acta Crystallogr., Sect. A*, **27**, 368 (1971).
(25) T. Debaerdemaeker and M. M. Woolfson, *Acta Crystallogr., Sect. A*, **28**, 477 (1972).
(26) R. Hoffmann, J. M. Howell, and E. Muetterties, *J. Am. Chem. Soc.*, **94**, 3047 (1972).
(27) A. Strich and A. Veillard, *J. Am. Chem. Soc.*, **95**, 5574 (1973).
(28) J. S. Szobota and R. R. Holmes, *Inorg. Chem.*, **16**, 2299 (1977). We have completed the X-ray structural investigation of the spirooxyphosphorane $[(CH_3)_2CO]_2P(OCC_6H_5)_2N(CH_3)_2$ and find the equatorial $(CH_3)_2N$ group with the C–N–C plane oriented 28° from the axial plane of the TP structure.
(29) A. Schmidpeter, J. Luber, D. Schomburg, and W. S. Sheldrick, *Chem. Ber.*, **109**, 3581 (1976).
(30) W. S. Sheldrick, *Acta Crystallogr., Sect. B*, **32**, 925 (1976).
(31) W. C. Hamilton, J. S. Ricci, Jr., F. Ramirez, L. Kramer, and P. Stern, *J. Am. Chem. Soc.*, **95**, 6335 (1973).
(32) (a) J. Wesley Cox and E. R. Corey, *Chem. Commun.*, 123 (1967); (b) A. Almenningen, B. Anderson, and E. E. Astrup, *Acta Chem. Scand.*, **23**, 2179 (1969); (c) L. G. Hoard and R. A. Jacobson, *J. Chem. Soc. A*, 1203 (1966); (d) H. Hess and D. Forst, *Z. Anorg. Allg. Chem.*, **342**, 240 (1966).

Contribution from the Department of Chemistry, University of Massachusetts, Amherst, Massachusetts 01003

Sterically Oriented Structures of Perfluoromethyl-Substituted Spirophosphoranes Centered between the Trigonal Bipyramid and the Rectangular Pyramid[1]

RICHARD K. BROWN,[2a] ROBERTA O. DAY, STEINAR HUSEBYE,[2b] and ROBERT R. HOLMES*

Received January 6, 1978

The crystal and molecular structures of 2,2,3,3-tetrakis(trifluoromethyl)-5-*tert*-butyl-7,8-benzo-1,4,6,9-tetraoxa-5λ^5-phosphaspiro[4.4]nonene, $(C_6H_4O_2)(O_2C_2(CF_3)_4)PC(CH_3)_3$, and 2,2,3,3-tetrakis(trifluoromethyl)-5-phenyl-7,8-benzo-1,4,6,9-tetraoxa-5λ^5-phosphaspiro[4.4]nonene, $(C_6H_4O_2)(O_2C_2(CF_3)_4)PC_6H_5$, have been determined by single-crystal X-ray diffraction analysis. The tertiary butyl derivative crystallizes in the monoclinic system (space group $P2_1/n$) with cell constants a = 12.285 (4) Å, b = 11.766 (5) Å, c = 14.116 (3) Å, β = 90.93 (3)°, and Z = 4. The structure was refined by full-matrix least squares to a final R value of 0.088 and a weighted R value of 0.086 for 3220 independent reflections with $F \geq \sigma(F)$. The molecular geometry is displaced 37% along the Berry intramolecular exchange coordinate. Pertinent features of the molecule relative to a rectangular pyramid are the diagonal O–P–O angles of 131.4 (2) and 164.3 (2)° and the four bond angles between the apical P–C bond of the *tert*-butyl group and the P–O bonds, 118.9 (3), 98.0 (2), 109.7 (7), and 97.5 (3)°. The differences in the P–O bond lengths, 1.709 (4) vs. 1.648 (4) Å for the perfluoropinacol residue and 1.684 (4) vs. 1.618 (4) Å for the benzo residue, are indicative of the trigonal-bipyramidal character. The phenyl derivative crystallizes in the monoclinic space group $C2/c$ with cell constants a = 18.108 (8) Å, b = 16.826 (7) Å, c = 14.593 (3) Å, and β = 112.71 (2)°. The structure was refined by full-matrix least squares to a final R value of 0.076 and a weighted R value of 0.062 for 2499 independent reflections with $F \geq 3\sigma(F)$. The molecular geometry is displaced 52% along the Berry intramolecular exchange coordinate. For this derivative, the diagonal O–P–O angles are 136.8 (2) and 161.3 (2)° and the four bond angles between the apical P–C bond of the phenyl group and the P–O bonds are 114.9 (2), 98.2 (2), 108.2 (2), and 100.5 (2)°. The differences in the P–O bond lengths, 1.685 (3) vs. 1.665 (3) Å for the perfluoropinacol groups and 1.668 (3) vs. 1.614 (3) Å for the benzo residue, again are indicative of trigonal-bipyramidal character. Conformational minimization shows that intermolecular effects are important in accounting for the smaller displacement along the Berry coordinate for the more sterically hindered *tert*-butyl derivative.

Introduction

Members of the spirocyclic phosphorane series I–VI[1b,3–7] exhibit solid-state structural distortions showing progressive displacement along the C_{2v} constraint of the Berry coordinate,[8] as measured by percent displacement[9] from the trigonal bipyramid toward the rectangular pyramid (given in parentheses). Similar measurements of structural distortions from X-ray studies[9–13] on related derivatives reveal the following factors favoring the formation of the rectangular pyramid: (1) increasing unsaturation in five-membered cyclic systems, (2) the presence of two such rings compared to the presence of one, (3) the presence of like atoms bonded to phosphorus in any one ring, (4) introduction of a more strained four-membered ring and, (5) the presence of an acyclic ligand in a spirocyclic derivative which is bulky and has low electro-

0020-1669/78/1317-3276$01.00/0 © 1978 American Chemical Society

Table I. Experimental Details of the X-ray Diffraction Studies of VII and VIII

	$(C_6H_4O_2)(O_2C_2(CF_3)_4)PC(CH_3)_3$ (VII)	$(C_6H_4O_2)(O_2C_2(CF_3)_4)PC_6H_5$ (VIII)
	(A) Crystal Data	
formula wt	528.3	548.3
space group	$P2_1/n$ [C_{2h}^5; No. 14][a]	$C2/c$ [C_{2h}^6; No. 15]
unit cell constants (22 ± 2 °C)	a = 12.285 (4) Å	a = 18.108 (8) Å
	b = 11.766 (5) Å	b = 16.826 (7) Å
	c = 14.116 (3) Å	c = 14.593 (3) Å
	β = 90.93 (3)°	β = 112.71 (2)°
	V = 2040.2 (6) Å^3	V = 4101 (1) Å^3
	Z = 4	Z = 8
	ρ(calcd) = 1.707 g cm^{-3}	ρ(calcd) = 1.777 g cm^{-3}
	ρ(obsd)[b] = 1.70 (3) g cm^{-3}	ρ(obsd)[b] = 1.75 (3) g cm^{-3}
	(B) Measurement of Intensity Data	
radiation	Mo Kα (Zr filtered); $\lambda_{K\alpha_1}$ 0.709 26 Å, $\lambda_{K\alpha_2}$ 0.713 54 Å	Mo Kα (graphite monochromator, $2\theta_m$ = 12.2°); $\lambda_{K\alpha_1}$ 0.709 26 Å, $\lambda_{K\alpha_2}$ 0.713 54 Å
attenuator	Zr foil	Zr foil
takeoff angle	3.50°	3.00°
detector receiving aperture	2-mm diameter	2-mm diameter
crystal-detector aperture distance	17.3 cm	17.3 cm
source-crystal distance	21.7 cm	21.7 cm
incident-beam collimator	1.3 mm	0.8 mm
scan type	ω-2θ	ω-2θ (recorded profiles)
scan speed	variable from 4.0 to 0.59°/min	variable from 4.0 to 0.11°/min
scan range	$\Delta\theta = (0.8 + 0.2 \tan\theta)°$	$\Delta\theta = (0.60 + 0.35 \tan\theta)°$
reflections measd	4596 in the region $+h, +k, \pm l$ with $2° \leqslant 2\theta \leqslant 60°$	3465 in the region $+h, +k, \pm l$ with $2° \leqslant 2\theta \leqslant 50°$
standard reflections	intensity controls (135, $\overline{135}$, 602, 250); measd every 50 reflections; no significant deviation from average was observed	intensity controls ($\overline{444}$, $\overline{444}$); measd every 12 000 s of exposure time; no significant deviation from average value was observed
background measurement	one quarter of scan time at beginning and end of 2θ scan	scan range was extended by 25% on each side of the scan for measurement of background, but actual values were determined from the recorded scan profiles using the Lehmann-Larsen algorithm[21]
	(C) Treatment of Intensity Data	
converstion to I and $\sigma(I)$	$I = [P - 2(B_1 + B_2)](FF/n_s)$, $\sigma(I) = [(P + 4(B_1 + B_2)(FF^2/n_s)) + (CI)^2]^{1/2}$[c]	$I = [P - (t_p/t_b)(B_1 + B_2)](FF/s)$, $\sigma(I) = [(P + (t_p/t_b)^2(B_1 + B_2)) + (CI)^2]^{1/2}(FF/s)$[c]
absorption correction[d]	μ(Mo Kα) = 2.63 cm^{-1}; grid 10 × 10 × 10; max and min transmission; factors 0.909 and 0.704	
extinction correction[d]	isotropic, of the form $F^{cor} = F_c(1 + 2gF_c^2\,\delta)^{-1/4}$ where $\delta = (e^2/mc^2V)^2(\lambda^3/\sin 2\theta)(p_2/p_1)\bar{T}$, $\bar{T}$ is the mean absorption weighted path length through the crystal for each reflection, $p_n = (1 + \cos^{2n} 2\theta)$ and V is the unit cell volume.	
	(D) Agreement Indices of Least-Squares Refinement	
k (scale factor)	0.4850 (6)	0.2235 (5)
g (isotropic extinction coefficient)		7.65 (9) × 10^2
n (no. of variables)	298	316
m (no. of intensities)	3220, $F \geqslant \sigma(F)$	2499, $F \geqslant 3\sigma(F)$
$R = (\Sigma\lvert F_o - F_c\rvert/\Sigma\lvert F_c\rvert)$	0.088	0.076
$R_w = (\Sigma w\lvert F_o - F_c\rvert^2/\Sigma wF_o^2)^{1/2}$	0.086	0.062
$S = [\Sigma w(F_o - F_c)^2/(m - n)]^{1/2}$	1.051	1.282

[a] $P2_1/n$ is a nonstandard setting for space group $P2_1/c$ and has the equipoints $\pm(x, y, z)$ and $\pm(^1/_2 + x, ^1/_2 - y, ^1/_2 + z)$. [b] Density as determined by the flotation method in a mixture of carbon tetrachloride and methyl iodide. [c] Variables are defined as follows: P, counts accumulated while scanning peak; B, counts accumulated while scanning background; n_s, scale factor inversely proportional to scan speed; FF, unity or attenuation factor for attenuator when inserted; t_p, time spent counting peak; t_b, time spent counting background; s, scale factor proportional to scan time. C was set equal to 0.045. [d] The absorption and extinction corrections listed apply to compound VII only.

negativity. Some of these trends may be seen to operate in the limited series I–VI outlined here.

In this paper, we present the structural analysis of the perfluorospirocyclic compounds VII and VIII. As will become apparent, the presence of the perfluoromethyl substituents on the saturated five-membered ring leads to a steric interaction suggesting the importance of intermolecular effects.

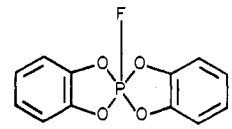

(65)
IV[5]

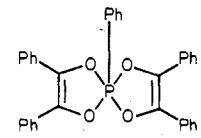

(82)
V[6]

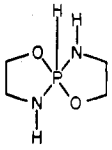

(25)
I[1b]

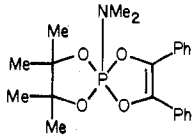

(31)
II[3]

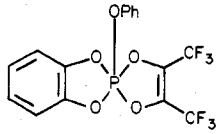

(57)
III[4]

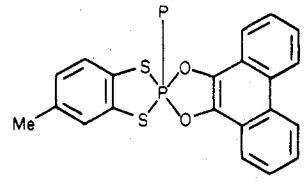

(93)
VI[7]

Table II. Final Positional Parameters for $(C_6H_4O_2)(O_2C_2(CF_3)_4)PC(CH_3)_3$[a]

atom	x	y	z
P	0.2642 (1)	0.6794 (1)	0.9745 (1)
O(1)	0.1784 (3)	0.7432 (3)	1.0455 (3)
O(2)	0.3634 (3)	0.7614 (3)	1.0261 (3)
O(3)	0.3453 (3)	0.5727 (3)	0.9914 (3)
O(4)	0.1590 (3)	0.5903 (4)	0.9546 (3)
CP(1)	0.2770 (6)	0.7318 (6)	0.8524 (4)
CP(2)	0.1725 (7)	0.7928 (7)	0.8218 (5)
CP(3)	0.3772 (7)	0.8069 (7)	0.8408 (4)
CP(4)	0.2903 (7)	0.6261 (7)	0.7903 (5)
C(1)	0.3416 (5)	0.8007 (5)	1.1164 (4)
C(2)	0.2159 (5)	0.8263 (5)	1.1096 (4)
C(3)	0.1849 (8)	0.9440 (6)	1.0641 (6)
C(4)	0.1484 (9)	0.8151 (9)	1.2021 (7)
C(5)	0.4198 (7)	0.9021 (7)	1.1388 (6)
C(6)	0.3723 (8)	0.7005 (7)	1.1877 (5)
C(7)	0.2960 (6)	0.4683 (5)	0.9831 (4)
C(8)	0.1889 (6)	0.4790 (6)	0.9641 (4)
C(9)	0.1170 (6)	0.3875 (8)	0.9568 (6)
C(10)	0.1728 (11)	0.2828 (8)	0.9697 (6)
C(11)	0.2806 (10)	0.2712 (7)	0.9869 (6)
C(12)	0.3440 (6)	0.3651 (7)	0.9954 (5)
F(31)	0.2452 (4)	0.9641 (3)	0.9893 (3)
F(32)	0.2010 (4)	1.0287 (4)	1.1240 (3)
F(33)	0.0836 (4)	0.9429 (4)	1.0371 (4)
F(41)	0.0519 (5)	0.8587 (5)	1.1915 (5)
F(42)	0.1379 (5)	0.7107 (5)	1.2287 (4)
F(43)	0.1961 (5)	0.8720 (5)	1.2715 (4)
F(51)	0.4221 (4)	0.9760 (4)	1.0712 (3)
F(52)	0.5209 (4)	0.8675 (5)	1.1508 (4)
F(53)	0.3917 (4)	0.9542 (4)	1.2165 (4)
F(61)	0.3036 (4)	0.6155 (4)	1.1784 (3)
F(62)	0.3764 (4)	0.7354 (4)	1.2752 (3)
F(63)	0.4714 (4)	0.6615 (4)	1.1659 (3)
H(21)	0.103	0.747	0.833
H(22)	0.155	0.865	0.846
H(23)	0.174	0.802	0.759
H(31)	0.346	0.874	0.862
H(32)	0.389	0.828	0.788
H(33)	0.399	0.882	0.875
H(41)	0.307	0.640	0.741
H(42)	0.361	0.571	0.819
H(43)	0.222	0.577	0.785
HC(9)	0.033	0.396	0.943
HC(10)	0.127	0.214	0.965
HC(11)	0.314	0.195	0.995
HC(12)	0.428	0.357	1.010

[a] Estimated standard deviations in parentheses.

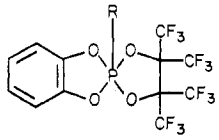

VII, R = *t*-Bu
VIII, R = Ph

These derivatives contain structural components corresponding to factors 1, 3, and 5 but lack components suggested by factors 2 and 4. Accordingly, an appropriate conformational balance[9,14] along the low-energy axial–equatorial bending coordinate[15] should be achieved at a point which is not near either idealized five-coordinated structure.

Experimental Section

Sample Preparation. Samples of 2,2,3,3-tetrakis(trifluoromethyl)-5-*tert*-butyl-7,8-benzo-1,4,6,9-tetraoxa-5λ^5-phosphaspiro[4.4]nonene (VII) and 2,2,3,3-tetrakis(trifluoromethyl)-5-phenyl-7,8-benzo-1,4,6,9-tetraoxa-5λ^5-phosphaspiro[4.4]nonene (VIII) were the generous gift of Dr. Gerd-Volker Roschenthaler, Technical University, Braunschweig, West Germany. Crystals of VII and VIII, suitable for detailed X-ray analyses, were obtained by recrystallization from methylene chloride and 1:1 methylene chloride–hexane solutions, respectively. All manipulations were carried out under a dry nitrogen atmosphere.

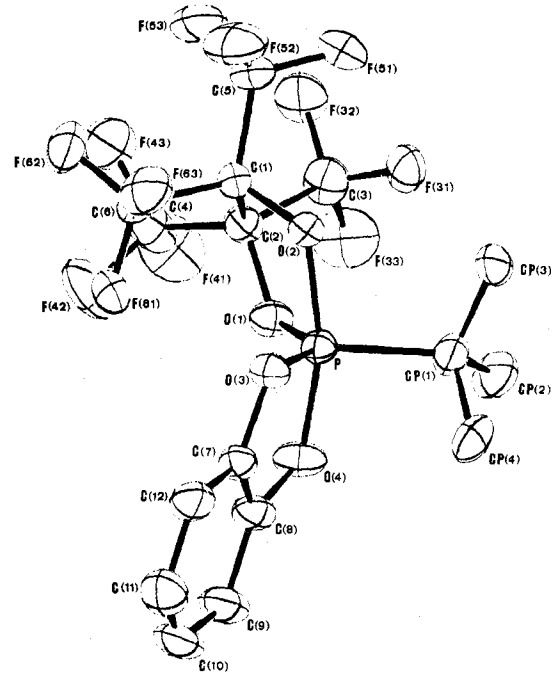

Figure 1. View of $(C_6H_4O_2)(O_2C_2(CF_3)_4)PC(CH_3)_3$, VII. Thermal ellipsoids are shown at the 50% probability level. The hydrogen atoms have been omitted.

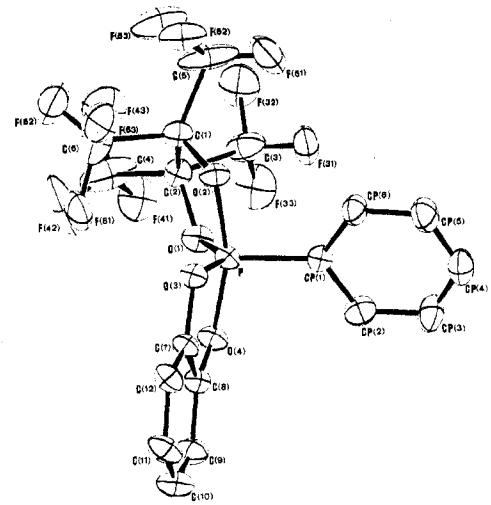

Figure 2. View of $(C_6H_4O_2)(O_2C_2(CF_3)_4)PC_6H_5$, VIII. Thermal ellipsoids are shown at the 50% probability level. The hydrogen atoms have been omitted.

Collection and Treatment of Data. Both compounds crystallize in the monoclinic system as well-formed rectangular platelets. A crystal of VII of dimensions 0.65 × 0.60 × 0.38 mm and a crystal of VIII of dimensions 0.35 × 0.40 × 0.55 mm were mounted in 0.7-mm glass capillaries. Each crystal was optically centered and randomly oriented on an Enraf-Nonius CAD-4 diffractometer equipped with a molybdenum X-ray tube and controlled by a PDP 8/e computer.

For VII, the unit cell constants and orientation matrix were determined from the angular settings of 15 high-order ($2\theta \geq 21.5°$) reflections. From the observed Laue symmetry ($2/m$) and the systematic absences, $0k0$ for $k = 2n + 1$ and $h0l$ for $h + l = 2n + 1$, the space group was uniquely determined as $P2_1/n$.

For VIII, the unit cell constants and orientation matrix were determined from the angular settings of 25 well-centered reflections in the range $15° \leq 2\theta \leq 43°$. From the observed Laue symmetry ($2/m$) and the systematic absences hkl for $h + k = 2n + 1$ and $h0l$ for $l = 2n + 1$, the space group was determined as either Cc or $C2/c$.

Table III. Thermal Parameters (Å) for $(C_6H_4O_2)(O_2C_2(CF_3)_4)PC(CH_3)_3$ with Standard Deviations in Parentheses[a]

atom	U_{11}	U_{22}	U_{33}	U_{12}	U_{13}	U_{23}
P	0.053 (1)	0.060 (1)	0.061 (1)	−0.001 (1)	−0.002 (1)	−0.001 (1)
O(1)	0.064 (3)	0.075 (3)	0.090 (3)	−0.006 (3)	0.006 (3)	−0.010 (3)
O(2)	0.064 (3)	0.061 (3)	0.066 (3)	−0.004 (3)	0.001 (3)	0.002 (3)
O(3)	0.063 (3)	0.062 (3)	0.082 (3)	0.001 (2)	−0.004 (2)	−0.003 (3)
O(4)	0.060 (3)	0.077 (4)	0.131 (4)	−0.003 (3)	−0.005 (3)	−0.021 (3)
CP(1)	0.106 (4)	0.091 (5)	0.061 (5)	0.005 (4)	−0.008 (4)	0.001 (4)
CP(2)	0.147 (6)	0.107 (6)	0.106 (6)	0.011 (5)	−0.053 (5)	0.012 (5)
CP(3)	0.162 (6)	0.094 (6)	0.066 (4)	−0.043 (4)	0.031 (4)	−0.005 (4)
CP(4)	0.167 (8)	0.133 (6)	0.054 (4)	−0.007 (4)	0.001 (4)	−0.018 (5)
C(1)	0.087 (4)	0.062 (4)	0.057 (4)	−0.008 (3)	−0.002 (3)	0.005 (3)
C(2)	0.085 (4)	0.065 (6)	0.073 (4)	−0.005 (4)	0.018 (4)	−0.009 (4)
C(3)	0.119 (6)	0.077 (6)	0.099 (5)	0.026 (5)	0.003 (5)	0.001 (5)
C(4)	0.170 (9)	0.099 (8)	0.131 (8)	−0.013 (8)	0.087 (8)	−0.017 (6)
C(5)	0.122 (5)	0.084 (5)	0.090 (6)	−0.033 (5)	−0.008 (5)	−0.017 (5)
C(6)	0.126 (6)	0.090 (6)	0.066 (5)	−0.008 (5)	−0.013 (5)	0.002 (4)
C(7)	0.082 (5)	0.056 (4)	0.070 (4)	−0.001 (4)	0.007 (4)	−0.009 (4)
C(8)	0.088 (5)	0.064 (5)	0.083 (5)	−0.009 (4)	0.016 (4)	−0.021 (4)
C(9)	0.127 (6)	0.075 (5)	0.121 (6)	−0.028 (5)	0.026 (5)	−0.022 (5)
C(10)	0.181 (9)	0.081 (6)	0.120 (6)	−0.064 (8)	0.044 (8)	−0.029 (5)
C(11)	0.158 (9)	0.083 (6)	0.114 (6)	−0.003 (6)	0.018 (6)	−0.006 (5)
C(12)	0.129 (6)	0.073 (5)	0.093 (5)	0.002 (5)	−0.011 (5)	−0.013 (4)
F(31)	0.164 (4)	0.071 (3)	0.087 (3)	0.015 (3)	−0.007 (3)	0.014 (3)
F(32)	0.208 (5)	0.066 (3)	0.129 (4)	0.019 (4)	0.023 (4)	−0.020 (3)
F(33)	0.118 (4)	0.138 (4)	0.217 (5)	0.059 (4)	−0.022 (4)	−0.005 (4)
F(41)	0.139 (4)	0.189 (6)	0.228 (6)	0.030 (5)	0.103 (5)	−0.015 (5)
F(42)	0.227 (6)	0.118 (4)	0.163 (5)	−0.032 (4)	0.122 (4)	0.004 (4)
F(43)	0.255 (6)	0.156 (5)	0.097 (4)	−0.048 (4)	0.070 (4)	−0.045 (4)
F(51)	0.157 (4)	0.099 (4)	0.128 (4)	−0.059 (3)	−0.002 (3)	0.013 (3)
F(52)	0.111 (4)	0.139 (4)	0.193 (5)	−0.026 (4)	−0.055 (3)	−0.014 (4)
F(53)	0.202 (5)	0.121 (4)	0.126 (4)	−0.061 (4)	0.016 (4)	−0.052 (4)
F(61)	0.162 (4)	0.076 (3)	0.089 (3)	−0.020 (3)	−0.001 (3)	0.021 (3)
F(62)	0.238 (5)	0.120 (4)	0.072 (3)	−0.007 (3)	−0.032 (4)	0.012 (3)
F(63)	0.134 (4)	0.118 (4)	0.132 (4)	0.015 (4)	−0.049 (3)	0.006 (3)

[a] The form of the anisotropic thermal ellipsoid is given by $\exp[(-\Sigma_i\Sigma_j h_i h_j - r_i^* r_j^* U_{ij})/4]$ where r_i^* is the ith reciprocal axis.

Successful refinement confirmed the space group as $C2/c$.

Corrections for Lorentz and polarization effects were made for both VII and VIII. Corrections for absorption and isotropic extinction were made for VII. The details of the experimental conditions, data collection, and treatment of intensity data for VII and VIII are given in Table I.

Structure Solution and Refinement. Computations were carried out on a CDC 6600 computer (Model Cyber 74-18) using local modifications of Zalkin's FORDAP Fourier program, Prewitt's SFLS-5 full-matrix least-squares routine, and various locally written programs. Scattering factors for all nonhydrogen atoms were taken from the tabulation by Cromer and Waber.[16] The hydrogen atom scattering factor used was that tabulated by Stewart.[17] The agreement factors are defined in Table I, part D. In all least-squares refinements, the quantity minimized was $\sum w(|F_o| - |F_c|)^2$. Weights were evaluated as $w^{1/2} = 2LpF_o/\sigma(I)$. For VII these weights proved to be unsatisfactory and were reevaluated as $w^{1/2} = 1/F_o$ for $F_o > 5.0$ and as $w^{1/2} = 0.20$ for $F_o \leq 5.0$.[18]

For VII, initial coordinates for all but three of the nonhydrogen atoms C(9), C(10), and C(11) were obtained from the phase-permutation program MULTAN.[19] After two cycles of isotropic unit weight refinement, a difference electron density map was calculated and found to reveal the position of the three remaining carbon atoms. Further isotropic unit weight refinement led to the values $R = 0.173$ and $R_w = 0.194$ for the 1949 reflections with $F \geq 4\sigma(F)$. Conversion was made to anisotropic temperature factors, and unit weight refinement was continued and led to values of 0.123 and 0.156 for R and R_w, respectively, for the 2631 reflections with $F \geq 2\sigma(F)$. This number of reflections was used in subsequent refinement except for the last cycle. It was obvious at this point in the refinement that extinction was severe, especially for the $h0l$ planes. Therefore an extinction correction, within the framework of the Zachariasen approximation,[20] was applied. A value of $7.65\ (9) \times 10^4$ was obtained for the isotropic extinction parameter. This led to $R = 0.096$ and $R_w = 0.110$. At this stage of refinement, a difference electron density map was again calculated and positions for the nine hydrogen atoms associated with the *tert*-butyl group were determined. Positions for the four hydrogen atoms associated with the catechol residue were calculated from the required geometry and a C–H bond distance of 1.0 Å. Refinement of the hydrogen atoms was unsatisfactory and their positions were fixed at the originally determined locations with isotropic temperature factors of $B = 5.0$ Å^2. Further anisotropic variable-weight refinement of the nonhydrogen atoms led to the final agreement indices shown in Table I, part D. A final difference Fourier map showed a peak of maximum intensity of 0.85 e/Å^3 at 0.275, 0.675, 0.975, a position very near the phosphorus atom. All other peaks were less than 0.57 e/Å^3. In the last cycle of least-squares refinement based on 3220 reflections with $F \geq \sigma(F)$, the largest shift in any parameter was less than 0.02 times its estimated standard deviation while the largest shift in any positional parameter was less than 0.006 times the associated standard deviation. The final positional and thermal parameters are presented in Tables II and III. For VIII, initial coordinates for the nonhydrogen atoms were obtained using MULTAN.[19] Three cycles of isotropic unit-weight refinement led to the values $R = 0.148$ and $R_w = 0.149$ for the 1236 reflections with $F > 8\sigma(F)$. Conversion was made to anisotropic temperature factors, and unit-weight refinement was continued for several cycles and led to values of 0.072 and 0.078 for R and R_w, respectively, based on the same set of reflections. Positions for the nine independent hydrogen atoms were calculated assuming a planar geometry and a C–H distance of 1 Å. The hydrogens were assigned isotropic temperature factors of $B = 5.0$ Å^2. Further anisotropic variable-weight refinement of the nonhydrogen atoms led to the final agreement indices shown in Table I, part D, which are based on the 2499 reflections with $F \geq 3\sigma(F)$. In the final cycle of least-squares refinement, the largest shift in any parameter was less than 0.16 times the associated standard deviation. A final difference electron density map revealed no peaks larger than 0.87 e/Å^3. The final positional and thermal parameters are presented in Tables IV and V.

Results and Discussion

Bond lengths and angles for $(C_6H_4O_2)(O_2C_2(CF_3)_4)PC(CH_3)_3$ (VII) and $(C_6H_4O_2)(O_2C_2(CF_3)_4)PC_6H_5$ (VIII) are listed in Tables VI and VII, respectively. Perspective views of VII and VIII are displayed in Figures 1 and 2. Corresponding schematic diagrams showing selected bond lengths and angles are presented in Figures 3 and 4, respectively.

Table IV. Final Positional Parameters for $(C_6H_4O_2)(O_2C_2(CF_3)_4)PC_6H_5$[a]

atom	x	y	z
P	0.68918 (7)	0.57859 (7)	−0.01018 (9)
O(1)	0.7887 (2)	0.5734 (2)	0.0418 (2)
O(2)	0.6912 (2)	0.4843 (2)	−0.0482 (2)
O(3)	0.6150 (2)	0.5506 (2)	0.0174 (2)
O(4)	0.7010 (2)	0.6575 (2)	0.0633 (2)
CP(1)	0.6498 (3)	0.6251 (3)	−0.1295 (3)
CP(2)	0.6526 (3)	0.7068 (3)	−0.1445 (5)
CP(3)	0.6203 (4)	0.7420 (4)	−0.2337 (5)
CP(4)	0.5855 (4)	0.6991 (4)	−0.3106 (4)
CP(5)	0.5788 (4)	0.6201 (4)	−0.3037 (4)
CP(6)	0.6099 (4)	0.5825 (3)	−0.2161 (4)
C(1)	0.7594 (3)	0.4409 (3)	−0.0124 (4)
C(2)	0.8308 (3)	0.5066 (3)	0.0343 (4)
C(3)	0.8605 (6)	0.5324 (5)	−0.0475 (8)
C(4)	0.9020 (4)	0.4884 (5)	0.1447 (9)
C(5)	0.7632 (4)	0.3843 (5)	−0.0968 (8)
C(6)	0.7528 (4)	0.3961 (6)	0.0852 (7)
C(7)	0.5870 (3)	0.6082 (3)	0.0663 (3)
C(8)	0.6395 (3)	0.6704 (3)	0.0876 (3)
C(9)	0.6246 (3)	0.7342 (3)	0.1387 (4)
C(10)	0.5600 (4)	0.7371 (4)	0.1562 (4)
C(11)	0.5063 (3)	0.6741 (4)	0.1322 (4)
C(12)	0.5222 (3)	0.6087 (3)	0.0834 (4)
F(31)	0.7928 (2)	0.5466 (3)	−0.1435 (3)
F(32)	0.9040 (2)	0.4809 (2)	−0.0705 (4)
F(33)	0.9023 (2)	0.5957 (3)	−0.0255 (3)
F(41)	0.9539 (2)	0.5516 (3)	0.1382 (3)
F(42)	0.8814 (3)	0.4877 (5)	0.2060 (3)
F(43)	0.9409 (2)	0.4296 (3)	0.1125 (3)
F(51)	0.7592 (4)	0.4147 (3)	−0.1684 (4)
F(52)	0.7119 (2)	0.3261 (2)	−0.0952 (3)
F(53)	0.8324 (3)	0.3388 (4)	−0.0410 (4)
F(61)	0.7457 (3)	0.4539 (3)	0.1507 (3)
F(62)	0.8102 (3)	0.3477 (3)	0.1282 (4)
F(63)	0.6861 (3)	0.3548 (2)	0.0485 (3)
HCP(2)	0.684	0.740	−0.078
HCP(3)	0.626	0.805	−0.240
HCP(4)	0.558	0.728	−0.382
HCP(5)	0.547	0.588	−0.366
HCP(6)	0.606	0.519	−0.210
HC(9)	0.666	0.786	0.159
HC(10)	0.546	0.784	0.195
HC(11)	0.458	0.676	0.148
HC(12)	0.480	0.558	0.065

[a] Estimated standard deviations in parentheses.

The molecular structures are intermediate between the trigonal bipyramid and the rectangular pyramid. Both appear along the C_{2v} constraint of the Berry coordinate.[8] On the basis of the sum of dihedral angles[9] obtained from the polytopal faces using observed bond lengths, the phenyl derivative (VIII) is centered between the two idealized geometries at a point 52% displaced from the trigonal bipyramid toward the rectangular pyramid. The same type of calculation applied to the *tert*-butyl derivative (VII) shows that the structure is distorted 37% from the trigonal bipyramid. For unit bond lengths, these values are 55 and 40%, respectively. These results are summarized in Table VIII.

The residual trigonal-bipyramidal character is evident from the magnitudes of the P–O bond distances. In both derivatives, the two P–O bonds associated with the benzo group show one longer and one shorter bond length. The "axial" distance in the *tert*-butyl derivative (VII), P–O(4) = 1.684 (4) Å, is significantly longer than the "equatorial" distance P–O(3) = 1.618 (4) Å. Likewise, in the phenyl derivative (VIII), P–O(4) (1.668 (3) Å) is longer than P–O(3) (1.614 (3) Å). A similar situation prevails for the P–O bonds associated with the perfluoropinacol residues. In both derivatives, an "axial" distance, P–O(2) = 1.709 (4) Å for VII and 1.685 (3) Å for VIII, opposite P–O(4), is longer than the "equatorial" distance,

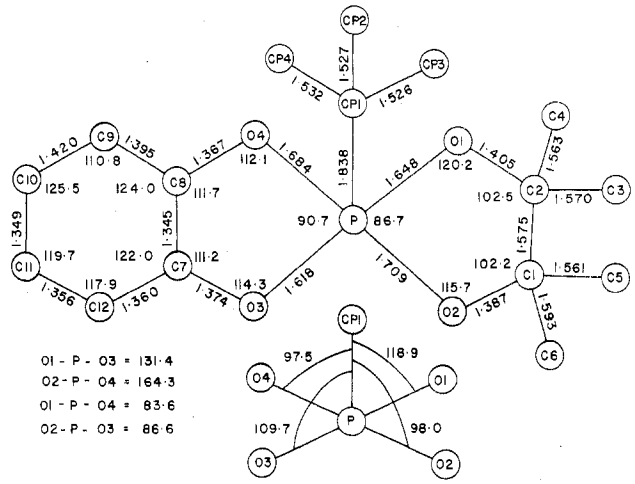

Figure 3. Schematic drawing of $(C_6H_4O_2)(O_2C_2(CF_3)_4)PC(CH_3)_3$, VII, showing bond distances (Å) and angles (deg).

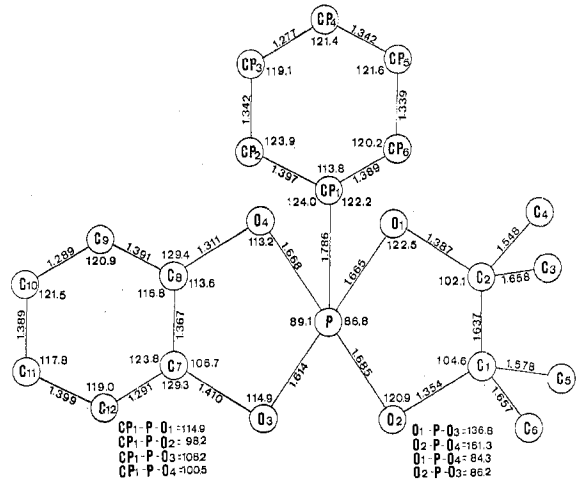

Figure 4. Schematic drawing of $(C_6H_4O_2)(O_2C_2(CF_3)_4)PC_6H_5$, VIII, showing bond distances (Å) and angles (deg).

P–O(1) = 1.648 (4) Å for VII and 1.665 (3) Å for VIII. Both also show the respective axial and equatorial distances associated with the benzo residue shorter than the corresponding axial and equatorial distances associated with the perfluoropinacol group. The same bond-length effect is noted in the related perfluoro compound[4]

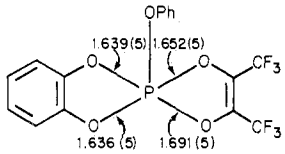

which is displaced 57% along the Berry coordinate. This observation is in contrast to the usual trend, at least in the case of the axial P–O bond lengths where sufficient information has been accumulated.[9,22] Normally, the five-membered ring containing an unsaturated component has longer P–O "axial" bonds relative to axial P–O bonds in saturated five-membered rings. For the degree of structural distortion reported here, the expected axial P–O bond distances for unsaturated five-membered rings should be 1.74 and 1.71 Å for VII and VIII, respectively, based on an analysis of related compounds.[9] Thus, the values obtained for these distances are shorter by 0.06 Å for the *tert*-butyl derivative and 0.04 Å for the phenyl derivative. For the saturated five-membered ring component, axial P–O bond lengths have been reported in the range 1.63–1.70 Å.[9,10] The values obtained here are at or are a little

Table V. Thermal Parameters (Å) for $(C_6H_4O_2)(O_2C_2(CF_3)_4)PC_6H_5$ with Standard Deviations in Parentheses[a]

atom	U_{11}	U_{22}	U_{33}	U_{12}	U_{13}	U_{23}
P	0.046 (1)	0.052 (1)	0.052 (1)	−0.011 (1)	−0.003 (1)	−0.006 (1)
O(1)	0.045 (2)	0.077 (2)	0.093 (2)	−0.012 (1)	−0.010 (1)	−0.022 (1)
O(2)	0.055 (2)	0.058 (2)	0.087 (2)	0.000 (1)	−0.015 (1)	−0.018 (1)
O(3)	0.059 (2)	0.052 (2)	0.063 (2)	−0.009 (1)	−0.007 (1)	−0.007 (1)
O(4)	0.056 (2)	0.071 (2)	0.070 (2)	−0.015 (1)	−0.001 (1)	−0.018 (1)
CP(1)	0.060 (3)	0.062 (4)	0.070 (3)	−0.013 (3)	−0.012 (3)	0.003 (3)
CP(2)	0.102 (5)	0.061 (4)	0.119 (5)	−0.026 (4)	−0.025 (4)	−0.011 (4)
CP(3)	0.171 (6)	0.077 (5)	0.095 (5)	−0.023 (5)	−0.020 (5)	0.047 (4)
CP(4)	0.114 (5)	0.123 (6)	0.061 (4)	0.015 (4)	−0.023 (4)	0.032 (4)
CP(5)	0.168 (6)	0.100 (5)	0.059 (4)	−0.016 (5)	−0.048 (4)	0.004 (4)
CP(6)	0.162 (6)	0.057 (3)	0.068 (4)	−0.017 (4)	−0.036 (4)	0.002 (3)
C(1)	0.050 (3)	0.080 (4)	0.106 (3)	0.008 (3)	0.001 (3)	−0.013 (4)
C(2)	0.060 (4)	0.069 (4)	0.092 (4)	−0.004 (3)	−0.007 (3)	0.005 (3)
C(3)	0.178 (10)	0.070 (5)	0.236 (11)	−0.014 (5)	0.093 (9)	−0.019 (6)
C(4)	0.046 (4)	0.116 (6)	0.289 (5)	0.027 (5)	−0.069 (6)	−0.061 (9)
C(5)	0.061 (5)	0.087 (6)	0.291 (13)	−0.006 (4)	0.033 (6)	−0.082 (8)
C(6)	0.059 (4)	0.159 (9)	0.177 (9)	−0.016 (5)	0.005 (5)	0.076 (6)
C(7)	0.047 (3)	0.062 (3)	0.060 (3)	−0.013 (3)	−0.008 (3)	−0.003 (3)
C(8)	0.046 (3)	0.064 (3)	0.071 (5)	0.003 (3)	−0.018 (3)	0.000 (3)
C(9)	0.072 (4)	0.071 (4)	0.095 (4)	−0.006 (3)	−0.005 (3)	−0.016 (3)
C(10)	0.087 (4)	0.087 (5)	0.102 (5)	0.014 (4)	−0.005 (4)	−0.020 (4)
C(11)	0.066 (4)	0.118 (5)	0.073 (4)	0.007 (4)	0.003 (3)	0.014 (4)
C(12)	0.060 (4)	0.084 (4)	0.075 (4)	−0.019 (3)	−0.012 (3)	−0.008 (3)
F(31)	0.122 (3)	0.168 (4)	0.073 (3)	0.049 (3)	0.002 (3)	0.040 (3)
F(32)	0.110 (4)	0.205 (5)	0.190 (5)	0.045 (3)	0.058 (4)	0.028 (6)
F(33)	0.102 (3)	0.182 (5)	0.174 (5)	−0.023 (4)	0.019 (4)	0.035 (4)
F(41)	0.067 (3)	0.179 (3)	0.133 (4)	−0.012 (3)	−0.046 (3)	0.003 (3)
F(42)	0.112 (4)	0.445 (10)	0.052 (3)	−0.014 (5)	−0.014 (3)	0.031 (4)
F(43)	0.091 (3)	0.192 (5)	0.172 (4)	−0.049 (3)	−0.033 (3)	−0.016 (4)
F(51)	0.355 (9)	0.165 (5)	0.097 (4)	−0.041 (5)	0.093 (5)	−0.019 (4)
F(52)	0.129 (4)	0.095 (3)	0.183 (4)	0.001 (3)	0.039 (4)	−0.048 (3)
F(53)	0.124 (4)	0.119 (4)	0.305 (8)	0.039 (3)	0.030 (4)	−0.044 (4)
F(61)	0.170 (4)	0.195 (5)	0.084 (3)	0.066 (4)	0.042 (3)	0.041 (3)
F(62)	0.175 (5)	0.133 (4)	0.149 (4)	0.040 (4)	0.009 (4)	0.052 (3)
F(63)	0.173 (5)	0.109 (4)	0.158 (4)	−0.017 (3)	0.026 (4)	0.033 (3)

[a] The form of the anisotropic thermal ellipsoid is given by $\exp[(-\Sigma_i\Sigma_j h_i h_j - r^*_i r^*_j U_{ij})/4]$ where r_i is the ith reciprocal axis.

greater than this upper range. As we shall discuss later on, a steric effect arises between the perfluoro groups and the unique ligand which is greater with the *tert*-butyl group. This no doubt causes some lengthening of the P–O(2) axial bonds in both derivatives. As a consequence of this bond-weakening effect, electron density may concentrate in the P–O bonds associated with the benzo residue leading to the shorter P–O(4) axial bond lengths that are observed.

The least-squares planes IV and V are rigorously satisfied for both the trigonal bipyramid and the rectangular pyramid. Following the local C_{2v} constraint imposed by the Berry coordinate, these planes should be closely adhered to. As shown in Table IX, this is found to be the case.

Plane III is a defining plane for an ideal rectangular pyramid while planes V and VI are defining planes for the trigonal bipyramid. Owing to the intermediacy of the structures along the Berry coordinate, sizable atom deviations from these planes are obtained (Table IX).

Regarding ring planarity, the atoms of the benzo rings for the *tert*-butyl derivative show an average out-of-plane variation of ±0.007 Å. This compares with a considerably larger variation of ±0.016 Å for this ring in the phenyl derivative (plane I, Table IX). The attached five-membered ring, similarly, shows a greater degree of planarity in the *tert*-butyl compound giving an average atom deviation of ±0.08 Å compared to ±0.076 Å for the phenyl compound (plane II). These results complement the relative shortening of the P–O(4) axial bond in the *tert*-butyl derivative discussed above in terms of increased electron density.

The saturated five-membered rings of the perfluoropinacol group show considerable puckering, more so with the *tert*-butyl derivative (plane VIII). The "flap" atom is C(1) in both cases with the direction of the atom pucker away from the unique ligand. This positioning minimizes any steric interaction of the perfuoromethyl groups attached to C(1) with either the *tert*-butyl methyl groups or the phenyl group. Both the *tert*-butyl methyl groups and the phenyl group are oriented so that they offer minimal interference with the CF_3 groups. The closest contact between a methyl carbon of the *tert*-butyl group and a fluorine atom is 3.22 (1) Å for CP(2)–F(31). The nearly planar phenyl group, plane IX of Table IX, exhibits a dihedral angle of 17.1° (Table X) with the axial P–O(2)–O(4)–CP(1) direction (plane IV). The direction of rotation, as seen in Figure 2, presumably is a result of minimizing steric interactions since the α carbon, CP(6), is rotated away from the CF_3 group positioned at C(3). Because of this ability of the equatorial phenyl group to lessen steric interactions by rotating out of the way in contrast to that in the *tert*-butyl derivative, the steric interaction between the *tert*-butyl group and the CF_3 group centered at C(3) is expected to be larger. The closest contact between the phenyl group and a fluorine atom is 3.123 (7) Å for CP(6)–F(31). Other dihedral angles of interest and intramolecular nonbonded distances which describe the molecular polyhedron are listed in Tables X and XI, respectively.

The perfluoromethyl groups centered at C(4) and C(5) in the phenyl derivative are disordered. The disorder does not appear to arise from simple rotation about the C–C bonds but rather from a translation of the entire CF_3 groups. Although the translation is slight, we were unable to resolve the disordered atoms. In the *tert*-butyl compound, slightly larger amplitudes of libration are also associated with the CF_3 groups.

Alternation in C–O bond lengths, similar to that observed in other ring-containing phosphoranes,[22] is present in these perfluoro compounds. The C–O bonds attached to the longer "axial" P–O bonds are shorter than the corresponding C–O bonds attached to the "equatorial" oxygen atoms. Also the tendency for a compression of angles at C(9) and C(12) below

Table VI. Bond Distances (Å) and Angles (deg) for $(C_6H_4O_2)(O_2C_2(CF_3)_4)PC(CH_3)_3$

Distances			
P-CP(1)	1.838 (6)	C(3)-F(32)	1.320 (9)
P-O(1)	1.648 (4)	C(3)-F(33)	1.296 (11)
P-O(2)	1.709 (4)	C(4)-F(41)	1.298 (12)
P-O(3)	1.618 (4)	C(4)-F(42)	1.293 (10)
P-O(4)	1.684 (4)	C(4)-F(43)	1.316 (12)
O(1)-C(2)	1.405 (7)	C(5)-F(51)	1.292 (9)
O(2)-C(1)	1.387 (7)	C(5)-F(52)	1.315 (10)
O(3)-C(7)	1.374 (8)	C(5)-F(53)	1.309 (10)
O(4)-C(8)	1.367 (8)	C(6)-F(61)	1.313 (9)
CP(1)-CP(2)	1.527 (9)	C(6)-F(62)	1.302 (8)
CP(1)-CP(3)	1.526 (9)	C(6)-F(63)	1.342 (10)
CP(1)-CP(4)	1.532 (9)	C(9)-HC(9)	1.05
C(1)-C(2)	1.575 (8)	C(10)-HC(10)	0.98
C(1)-C(5)	1.561 (9)	C(11)-HC(11)	1.00
C(1)-C(6)	1.593 (9)	C(12)-HC(12)	1.05
C(2)-C(4)	1.563 (11)	CP(2)-H(21)	1.03
C(2)-C(3)	1.570 (9)	CP(2)-H(22)	0.94
C(7)-C(8)	1.345 (9)	CP(2)-H(23)	0.90
C(8)-C(9)	1.395 (9)	CP(3)-H(31)	0.93
C(9)-C(10)	1.420 (11)	CP(3)-H(32)	0.80
C(10)-C(11)	1.349 (12)	CP(3)-H(33)	1.04
C(11)-C(12)	1.356 (9)	CP(4)-H(41)	0.80
C(12)-C(7)	1.360 (9)	CP(4)-H(42)	1.16
C(3)-F(31)	1.320 (10)	CP(4)-H(43)	1.02

Angles			
CP(1)-P-O(1)	118.9 (3)	P-O(1)-C(2)	120.2 (4)
CP(1)-P-O(2)	98.0 (2)	P-O(2)-C(1)	115.7 (3)
CP(1)-P-O(3)	109.7 (7)	P-O(3)-C(7)	114.3 (4)
CP(1)-P-O(4)	97.5 (3)	P-O(4)-C(8)	112.1 (4)
O(1)-P-O(2)	86.7 (2)	O(1)-C(2)-C(1)	102.5 (5)
O(2)-P-O(3)	86.6 (2)	C(2)-C(1)-O(2)	102.2 (4)
O(3)-P-O(4)	90.7 (2)	O(3)-C(7)-C(8)	111.2 (6)
O(1)-P-O(4)	83.6 (2)	C(7)-C(8)-O(4)	111.7 (6)
O(1)-P-O(3)	131.4 (2)	O(3)-C(7)-C(12)	126.7 (6)
O(2)-P-O(4)	164.3 (2)	O(4)-C(8)-C(9)	124.3 (6)
P-CP(1)-CP(2)	109.8 (5)	C(7)-C(8)-C(9)	124.0 (6)
P-CP(1)-CP(3)	112.1 (4)	C(8)-C(9)-C(10)	110.8 (7)
P-CP(1)-CP(4)	106.0 (4)	C(9)-C(10)-C(11)	125.5 (8)
CP(2)-CP(1)-CP(3)	111.9 (5)	C(10)-C(11)-C(12)	119.7 (8)
CP(2)-CP(1)-CP(4)	108.5 (6)	C(11)-C(12)-C(7)	117.9 (7)
CP(3)-CP(1)-CP(4)	108.3 (5)	C(12)-C(7)-C(8)	122.0 (6)
O(1)-C(2)-C(3)	106.0 (5)	C(2)-C(3)-F(32)	111.8 (7)
O(1)-C(2)-C(4)	107.9 (6)	C(2)-C(3)-F(33)	109.7 (7)
O(2)-C(1)-C(5)	108.3 (5)	C(2)-C(4)-F(41)	111.5 (8)
O(2)-C(1)-C(6)	106.7 (5)	C(2)-C(4)-F(42)	112.3 (8)
C(3)-C(2)-C(4)	106.7 (6)	C(2)-C(4)-F(43)	110.1 (8)
C(5)-C(1)-C(6)	107.4 (5)	F(31)-C(3)-F(32)	107.2 (7)
C(1)-C(2)-C(3)	115.1 (5)	F(31)-C(3)-F(33)	108.4 (7)
C(1)-C(2)-C(4)	117.7 (6)	F(32)-C(3)-F(33)	109.1 (7)
C(2)-C(1)-C(5)	117.8 (5)	F(41)-C(4)-F(42)	108.2 (8)
C(2)-C(1)-C(6)	113.7 (5)	F(41)-C(4)-F(43)	106.2 (8)
C(1)-C(5)-F(51)	112.7 (7)	F(42)-C(4)-F(43)	108.2 (8)
C(1)-C(5)-F(52)	111.6 (7)	F(51)-C(5)-F(52)	105.8 (7)
C(1)-C(5)-F(53)	111.0 (7)	F(51)-C(5)-F(53)	108.2 (7)
C(1)-C(6)-F(61)	110.8 (6)	F(52)-C(5)-F(53)	107.3 (7)
C(1)-C(6)-F(62)	111.8 (6)	F(61)-C(6)-F(62)	110.5 (6)
C(1)-C(6)-F(63)	108.4 (6)	F(61)-C(6)-F(63)	107.5 (6)
C(2)-C(3)-F(31)	110.5 (6)	F(62)-C(6)-F(63)	107.7 (6)

Table VII. Bond Distances (Å) and Angles (deg) for $(C_6H_4O_2)(O_2C_2(CF_3)_4)PC_6H_5$

Distances			
P-CP(1)	1.786 (5)	C(11)-C(12)	1.399 (8)
P-O(1)	1.665 (3)	C(12)-C(7)	1.291 (6)
P-O(2)	1.685 (3)	C(3)-F(31)	1.482 (11)
P-O(3)	1.614 (3)	C(3)-F(32)	1.300 (10)
P-O(4)	1.668 (3)	C(3)-F(33)	1.273 (12)
O(1)-C(2)	1.387 (6)	C(4)-F(41)	1.447 (9)
O(2)-C(1)	1.354 (6)	C(4)-F(42)	1.094 (12)
O(3)-C(7)	1.410 (5)	C(4)-F(43)	1.398 (10)
O(4)-C(8)	1.311 (5)	C(5)-F(51)	1.141 (12)
CP(1)-CP(2)	1.397 (5)	C(5)-F(52)	1.356 (9)
CP(2)-CP(3)	1.342 (9)	C(5)-F(53)	1.426 (9)
CP(3)-CP(4)	1.277 (9)	C(6)-F(61)	1.403 (11)
CP(4)-CP(5)	1.342 (10)	C(6)-F(62)	1.278 (11)
CP(5)-CP(6)	1.339 (8)	C(6)-F(63)	1.315 (11)
CP(6)-CP(1)	1.389 (7)	C(9)-HC(9)	1.12
C(1)-C(2)	1.637 (7)	C(10)-HC(10)	1.06
C(1)-C(5)	1.578 (12)	C(11)-HC(11)	0.99
C(1)-C(6)	1.657 (11)	C(12)-HC(12)	1.10
C(2)-C(3)	1.658 (12)	CP(2)-HCP(2)	1.07
C(2)-C(4)	1.548 (12)	CP(3)-HCP(3)	1.08
C(7)-C(8)	1.367 (6)	CP(4)-HCP(4)	1.08
C(8)-C(9)	1.391 (7)	CP(5)-HCP(5)	1.03
C(9)-C(10)	1.289 (8)	CP(6)-HCP(6)	1.07
C(10)-C(11)	1.389 (8)		

Angles			
CP(1)-P-O(1)	114.9 (2)	C(2)-C(1)-O(2)	104.6 (4)
CP(1)-P-O(2)	98.2 (2)	O(3)-C(7)-C(8)	106.7 (4)
CP(1)-P-O(3)	108.2 (2)	C(7)-C(8)-O(4)	113.6 (4)
CP(1)-P-O(4)	100.5 (2)	O(3)-C(7)-C(12)	129.3 (4)
O(1)-P-O(2)	86.8 (2)	O(4)-C(8)-C(9)	129.4 (5)
O(2)-P-O(3)	86.2 (2)	C(7)-C(8)-C(9)	116.8 (4)
O(3)-P-O(4)	89.1 (2)	C(8)-C(9)-C(10)	120.9 (5)
O(1)-P-O(4)	84.3 (2)	C(9)-C(10)-C(11)	121.5 (6)
O(1)-P-O(3)	136.8 (2)	C(10)-C(11)-C(12)	117.8 (6)
O(2)-P-O(4)	161.3 (2)	C(11)-C(12)-C(7)	119.0 (5)
P-CP(1)-CP(2)	124.0 (4)	C(12)-C(7)-C(8)	123.8 (5)
P-CP(1)-CP(6)	122.2 (4)	O(1)-C(2)-C(3)	101.5 (4)
CP(1)-CP(2)-CP(3)	123.9 (5)	O(1)-C(2)-C(4)	108.5 (5)
CP(2)-CP(3)-CP(4)	119.1 (6)	O(2)-C(1)-C(5)	109.5 (5)
CP(3)-CP(4)-CP(5)	121.4 (7)	O(2)-C(1)-C(6)	102.6 (5)
CP(4)-CP(5)-CP(6)	121.6 (6)	C(3)-C(2)-C(4)	115.5 (5)
CP(5)-CP(6)-CP(1)	120.2 (5)	C(5)-C(1)-C(6)	115.8 (5)
CP(6)-CP(1)-CP(2)	113.8 (5)	C(1)-C(2)-C(3)	108.8 (5)
P-O(1)-C(2)	122.5 (3)	C(2)-C(3)-F(33)	113.0 (6)
P-O(2)-C(1)	120.9 (3)	C(2)-C(4)-F(41)	94.7 (6)
P-O(3)-C(7)	114.9 (3)	C(2)-C(4)-F(42)	114.5 (8)
P-O(4)-C(8)	113.2 (3)	C(2)-C(4)-F(43)	96.1 (6)
O(1)-C(2)-C(1)	102.1 (4)	F(31)-C(3)-F(32)	103.0 (6)
C(1)-C(2)-C(4)	118.2 (5)	F(31)-C(3)-F(33)	107.3 (6)
C(2)-C(1)-C(5)	117.8 (5)	F(32)-C(3)-F(33)	105.2 (6)
C(2)-C(1)-C(6)	104.9 (5)	F(41)-C(4)-F(42)	119.9 (9)
C(1)-C(5)-F(51)	116.0 (7)	F(41)-C(4)-F(43)	94.2 (6)
C(1)-C(5)-F(52)	100.7 (6)	F(42)-C(4)-F(43)	130.0 (9)
C(1)-C(5)-F(53)	100.0 (6)	F(51)-C(5)-F(52)	122.5 (8)
C(1)-C(6)-F(61)	109.1 (6)	F(51)-C(5)-F(53)	119.6 (7)
C(1)-C(6)-F(62)	113.5 (7)	F(52)-C(5)-F(53)	93.4 (6)
C(1)-C(6)-F(63)	104.5 (6)	F(61)-C(6)-F(62)	112.2 (7)
C(2)-C(3)-F(31)	111.5 (5)	F(61)-C(6)-F(63)	109.4 (7)
C(2)-C(3)-F(32)	115.9 (6)	F(62)-C(6)-F(63)	108.0 (9)

120° and an expansion at C(7) and C(8) above 120° in the six-membered ring of the benzo residue is evident, particularly in the *tert*-butyl derivative. These bond-length and -angle alternations have been attributed to secondary effects resulting from the considerable difference in axial vs. equatorial bonding in a trigonal bipyramid.[11,22]

Using the electron-pair-repulsion model,[23] the less electronegative *tert*-butyl group would place electron density closer to phosphorus in the P–CP(1) bond compared to this effect with a phenyl group. As a consequence, distortion toward the rectangular pyramid would be favored since the electron pairs in nearby "axial" bonds would experience a large repulsion and undergo movement to open up the axial–equatorial angle from 90 toward 105°.[24] A steric effect exerted by the unique equatorial ligand would appear to also favor the formation of a rectangular-pyramidal structure for a spirocyclic derivative.

This seems to be the case in related oxyphosphoranes. Thus, in the dibenzo spirocyclic series

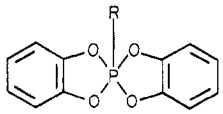

with R = H,[25] F (65),[5] Cl (72),[13] Ph (72),[11] adamantyl (73),[26] Me (82)[27], *t*-Bu (84),[28] and OPh (88),[29] the trend in displacement along the Berry coordinate toward the rectangular pyramid (shown as percent displacement in parentheses) follows general expectations based on a mixture of an elec-

Table VIII. Dihedral Angles for $(C_6H_4O_2)PR(O_2C_2(CF_3)_4)$ (deg)[a]

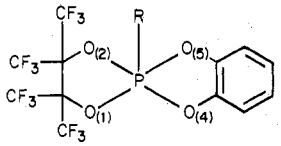

edge[b]	R = *t*-Bu A[e]	R = *t*-Bu B[e]	R = Ph A	R = Ph B
45	102.1	103.8	106.7	108.3
25	109.9	111.0	112.3	113.0
14	104.1	105.4	106.9	108.3
12	109.4	110.0	110.9	111.4
35	93.9	91.6	88.7	87.1
13	93.6	90.9	89.4	87.4
23	59.4	58.7	65.0	64.0
34	68.6	68.3	70.0	69.9
24	29.8	31.5	22.8	23.6
$\Sigma_i\lvert\delta_i(C) - \delta_i(TP)\rvert$	80.0	87.1	114.0	120.7
$\Sigma_i\lvert\delta_i(C) - \delta_i(RP)\rvert$	137.6	130.6	105.4	97.0
$R - \Sigma_i\lvert\delta_i(C) - \delta_i(RP)\rvert$[c]	80.1	87.1	112.3	120.7
% along Berry coord[d]	37	40	52	55

[a] See ref 9 for a more complete discussion of this method. For purposes of comparison with a similar tabulation of dihedral angles for other compounds,[9] the atom-numbering scheme shown above is used where the subscripts 1 and 5 refer to axial-type atoms, 2 and 4 refer to equatorial-type atoms, and 3 refers to the equatorial-pivotal atom in the Berry process. [b] The number pairs refer to the common edge connecting the two triangular faces whose normals give the dihedral angle. [c] $R = \Sigma_i\lvert\delta_i(TP) - \delta_i(RP)\rvert = 217.7°$. This value represents the sum of dihedral angle changes on going from the idealized trigonal bipyramid (TP) to the idealized rectangular pyramid (RP). The close adherence to the Berry coordinate is shown by the near equality of the sums $\Sigma_i\lvert\delta_i(C) - \delta_i(TP)\rvert$ and $R - \Sigma_i\lvert\delta_i(C) - \delta_i(RP)\rvert$. Refer to Table III of ref 9 for the values of the dihedral angles for the idealized TP and RP. [d] Percent displacement along the Berry coordinate from the trigonal bipyramid toward the rectangular pyramid. [e] Column A represents dihedral angles calculated from the actual bond distances. Column B shows dihedral angles calculated using unit bond lengths.

tronegativity effect and a steric contribution.[10,13] The OPh, owing to the angle at oxygen, probably has the largest steric effect placing it out-of-order on an electronegativity basis. The opposite situation prevails for the proton, while the phenyl and *tert*-butyl groups appear to show relatively modest steric effects. As pointed out above, a steric effect is encountered, principally between the CF_3 group at C(3) and the equatorial substituent, which appears greater for the *tert*-butyl derivative. It is then somewhat surprising to find the phenyl derivative (VIII), reported here, displaced along the Berry coordinate farther than the *tert*-butyl derivative (VII), an order opposite to that observed in the dibenzo series.

To probe the nature of the steric terms encountered in these highly substituted perfluoromethyl spirophosphoranes, we carried out conformational minimization calculations based on the well-developed molecular mechanics program MMI of Allinger et al.,[30,31] suitably modified to treat phosphoranes.[14]

The two derivatives were at first treated as independent molecules. The calculations were then repeated with the molecules placed in their respective unit cell environments in order to estimate the effect of intermolecular interactions. In performing these calculations, the X-ray coordinates were initially used to define the geometry. To allow easy slippage along the Berry coordinate, as previously found in solid-state phosphorane structures,[9] the force constants for angle bending for all angles at phosphorus were set to zero. In addition, the "strainless" parameters characterizing the idealized trigonal-bipyramidal structure were assumed.[32]

As observed in the present X-ray structures, as well as those in the dibenzo series, the $PO_2C_6H_4$ moiety is very close to

Table IX. Atom Distances from Least-Squares Planes for $(C_6H_4O_2)PR(O_2C_2(CF_3)_4)$ (Å)[a]

plane	R	atoms and deviations					
I		C(7)	C(8)	C(9)	C(10)	C(11)	C(12)
	t-Bu	0.002	−0.008	0.009	0.003	−0.014	0.007
	Ph	0.018	−0.025	0.026	−0.014	0.003	−0.009
II		P	O(3)	C(7)	C(8)	O(4)	
	t-Bu	0.001	−0.002	−0.006	0.020	−0.009	
	Ph	−0.015	0.079	−0.082	−0.110	0.094	
III		O(1)	O(2)	O(3)	O(4)	P[b]	
	t-Bu	0.242	−0.179	0.205	−0.268	−0.448	
	Ph	0.186	−0.172	0.146	−0.160	−0.437	
IV		P	O(2)	CP(1)	O(4)		
	t-Bu	−0.018	0.016	−0.009	0.025		
	Ph	−0.008	0.009	−0.002	0.008		
V		P	O(1)	CP(1)	O(3)		
	t-Bu	−0.001	0.001	0.001	0.000		
	Ph	0.007	−0.005	−0.006	−0.004		
VI		P	O(1)	O(2)	O(4)		
	t-Bu	−0.067	−0.092	0.088	0.133		
	Ph	−0.090	−0.120	0.151	0.143		
VII		P	O(2)	O(3)	O(4)		
	t-Bu	−0.093	0.107	−0.088	0.161		
	Ph	−0.108	0.161	−0.101	0.151		
VIII		P	O(1)	C(2)	C(1)	O(2)	
	t-Bu	0.013	−0.025	−0.141	0.310	−0.127	
	Ph	0.003	−0.001	−0.081	0.148	−0.056	
IX		CP(1)	CP(2)	CP(3)	CP(4)	CP(5)	CP(6)
	Ph	−0.003	0.001	0.006	−0.009	0.003	0.002

[a] The form of the least-squares plane is $lX + mY + nZ + d = 0$ where X, Y, and Z are orthogonal coordinates with Y and Z coincident with the crystal axes. The weights used for the ith atom are $w_i = 1/(a\sigma_x b\sigma_y c\sigma_z)^{2/3}$. [b] This atom was not included in the calculation of the least-squares plane.

Table X. Dihedral Angles between Some Least-Squares Planes for $(C_6H_4O_2)PR(O_2C_2(CF_3)_4)$ (deg)

planes[a]	R *t*-Bu	R Ph	planes[a]	R *t*-Bu	R Ph
I, II	177.7	171.8	VI, V	92.1	90.1
VI, VII	130.8	136.1	VII, V	90.6	91.3
IV, VI	120.0	116.1	IV, IX		17.1
IV, VII	109.2	107.8	V, IX		71.6
IV, V	88.1	88.6			

[a] Planes are as defined in Table IX.

Table XI. Selected Intramolecular Nonbonded Distances for $(C_6H_4O_2)PR(O_2C_2(CF_3)_4)$ (Å)

atoms	R *t*-Bu	R Ph	atoms	R *t*-Bu	R Ph
CP(1)–O(1)	3.005 (7)	2.911 (6)	O(2)–O(3)	2.283 (5)	2.254 (7)
CP(1)–O(2)	2.679 (7)	2.625 (6)	O(1)–O(3)	2.977 (5)	3.050 (7)
CP(1)–O(3)	2.830 (8)	2.757 (6)	O(1)–O(4)	2.221 (6)	2.237 (7)
CP(1)–O(4)	2.650 (8)	2.656 (6)	O(2)–O(4)	3.361 (6)	3.308 (7)
O(1)–O(2)	2.304 (5)	2.301 (7)	O(3)–O(4)	2.349 (5)	2.304 (7)

planarity; e.g., compare planes I and II (Table IX) and the dihedral angle between them (Table X). Accordingly, in the conformational treatment, the coordinates of benzene ring carbon atoms for the *tert*-butyl derivative were held constant relative to one another, whereas the two oxygen atoms of the benzo unit were allowed to move "freely" in the plane defined by their location and the coordinates for the benzene ring carbon atom bonded to the "equatorial" oxygen, i.e., one of the two oxygen atoms of the benzo unit. For the less sterically hindered phenyl compound, planarity of the $PO_2C_6H_4$ moiety was maintained without imposing the latter constraint. However, it was then necessary to constrain the movement of the P, O(1), O(3), and CP(1) atoms to a common plane.

To study the effects of intermolecular interactions, all atoms

Table XII. Comparison of the Bond Parameters at Phosphorus for $(C_6H_4O_2)(O_2C_2(CF_3)_4)PR$ Obtained by X-ray Diffraction and Conformational Minimization[a]

	R = *t*-Bu (VII)			R = Ph (VIII)		
	X-ray	calcd[b]	calcd(intermolc)[c]	X-ray	calcd[b]	calcd(intermolc)[c]
		Bond Distances, Å				
P–CP(1)	1.838	1.798	1.803	1.786	1.783	1.795
P–O(1)	1.648	1.637	1.637	1.665	1.632	1.634
P–O(2)	1.709	1.687	1.688	1.685	1.691	1.700
P–O(3)	1.618	1.633	1.633	1.614	1.633	1.629
P–O(4)	1.684	1.689	1.692	1.668	1.683	1.680
		Bond Angles, deg				
CP(1)–P–O(1)	118.9	114.3	122.3	114.9	113.4	121.5
CP(1)–P–O(2)	98.0	108.6	103.4	98.2	97.7	95.7
CP(1)–P–O(3)	109.7	104.1	107.3	108.2	107.4	103.8
CP(1)–P–O(4)	97.5	100.3	96.2	100.5	98.9	100.2
O(1)–P–O(2)	86.7	93.5	94.3	86.8	95.2	92.4
O(2)–P–O(3)	86.6	78.5	82.2	86.2	77.8	81.1
O(3)–P–O(4)	90.7	91.2	90.8	89.1	91.6	91.6
O(1)–P–O(4)	83.6	77.5	76.0	84.3	83.6	82.4
O(1)–P–O(3)	131.4	141.2	129.4	136.8	139.2	134.7
O(2)–P–O(4)	164.3	150.8	160.3	161.3	162.4	163.7
% along Berry coord[d,e]	37 (40)	77 (80)	41 (46)	52 (55)	54 (57)	45 (47)

[a] See text for a discussion of constraints and "strainless" parameters upon which these calculations were based. The value of the parameter *D* measuring the magnitude of the bond electron-pair-repulsion term was 0.1 for both derivatives.[14] [b] This column for each derivative refers to conformational calculations for which intermolecular interactions were excluded. [c] This column lists bond parameters calculated with the inclusion of intermolecular interactions (see text). [d] Percent displacement along the Berry coordinate from the trigonal bipyramid toward the rectangular pyramid as measured by the dihedral angle method.[9] [e] The unparenthesized values are obtained from dihedral angles using the X-ray or computed bond distances, as the case may be, and the parenthesized values are based on unit bond distances.[9]

in neighboring molecules in the unit cell closer than the sum of the van der Waals radii plus 0.6 Å to an atom in the original molecule were located. The coordinates of these neighbor atoms were held fixed during the conformational calculation and their van der Waals interactions with atoms in the initial molecule were included in determining the minimum-energy structure.

The general structural features were reproduced whether or not intermolecular effects were included in the calculations. Puckering occurred in the saturated five-membered ring at C(1) in the direction away from the equatorial substituent for both the phenyl and *tert*-butyl derivatives in agreement with the X-ray results. In the former derivative, the rotation of the phenyl group is in the direction shown by the X-ray results with closer agreement when intermolecular interactions are taken into consideration.

As measured by the percent displacement along the Berry coordinate (TP → RP), the minimum-energy structure for the *tert*-butyl derivative, without intermolecular interactions, was displaced further toward the rectangular pyramid (77%) than that for the phenyl derivative (54%). This order agrees with the order obtained for these two substituents in the dibenzo spirocyclic series, cited above, where intermolecular effects in general do not appear to be of major importance.

In the second calculation, with the inclusion of intermolecular interactions, the structural displacement of the *tert*-butyl derivative was reduced to 41%, near that for the actual X-ray structure, 37%. In contrast, a much smaller displacement took place for the phenyl derivative, from 54 to 45% as measured from the changes in dihedral angles based on the minimized bond lengths. A similar comparison results if changes in dihedral angles are based on unit bond lengths. The bond parameters at phosphorus for minimized structures, calculated with and without packing effects, are summarized in Table XII. Also, the bond parameters are compared with those obtained from the X-ray analysis of these two perfluoromethyl spirophosphoranes.

While the average bond angle deviation relative to the X-ray values for the phenyl derivative is about ±3° with and without the inclusion of intermolecular effects, a large improvement in structural comparison results for the *tert*-butyl derivative when intermolecular interactions are included ±4° (relative to ±7° without intermolecular effects). In the *tert*-butyl compound, there are strong intermolecular interactions between the two CF_3 groups on C(1) and proton and fluorine atoms on neighboring molecules. In minimizing these interactions, the movement of the pinacol carbon C(1) and associated ring atoms is in a direction which causes the axial angle O(2)–P–O(4) to increase toward 180°, i.e., toward the *tert*-butyl group. Other strong interactions are found between the *tert*-butyl protons and atoms of neighboring molecules but they are in directions more or less opposing each other. However, the *tert*-butyl group will be affected by the above movement of the pinacol ligand in determining the final minimum-energy structure.

As observed in other examples,[1b,3,9,22] relief of ring strain by puckering in saturated five-membered rings, as with that associated with the perfluoropinacol system, is a factor favoring less distortion toward the rectangular pyramid.[22] This effect alone accounts for the reduction in displacement of the phenyl derivative (VIII) of the perfluoropinacol series (52%) compared to that (72%) in the dibenzo series. For the *tert*-butyl derivative (VII) in the perfluoropinacol series, in addition to the latter ring puckering effect, the specific intermolecular packing effect encountered with this more sterically hindered structure causes further displacement toward the trigonal bipyramid. Thus, the much lower displacement from the trigonal bipyramid for the *tert*-butyl derivative (VII) (37%) relative to that for the *tert*-butyl compound in the dibenzo series (84%) is reasonably explained.

Acknowledgment. The support for this research by the National Science Foundation (Grant MPS 74-11496) and the National Institutes of Health (Grant GM 21466) and the inclusion of funds by NSF for the purchase of an Enraf-Nonius CAD-4 diffractometer are gratefully acknowledged. We thank the University of Massachusetts Computing Center for generous allocation of computer time. S.H. expresses his gratitude to the Norwegian Research Council for Science and the Humanities for a grant which aided this work.

Registry No. VII, 67462-97-9; VIII, 67425-71-2.

Supplementary Material Available: A compilation of observed and calculated structure factor amplitudes (50 pages). Ordering information is given on any current masthead page.

References and Notes

(1) (a) Part 31 of the series "Pentacoordinated Molecules." Presented in part at the 175th National Meeting of the American Chemical Society, Anaheim, Calif., March, 1978; Abstract No. INOR 196. (b) Part 30: P. F. Meunier, R. O. Day, J. R. Devillers, and R. R. Holmes, *Inorg. Chem.*, preceding paper in this issue.
(2) (a) This work in part represents a portion of the Ph.D. thesis of Richard K. Brown, University of Massachusetts, Amherst, Mass. (b) Visiting Professor at the University of Massachusetts, 1977–78, from the Chemical Institute, University of Bergen, Norway.
(3) J. S. Szobota and R. R. Holmes, *Inorg. Chem.*, **16**, 2299 (1977).
(4) P. Narayaman, H. M. Berman, F. Ramirez, J. F. Maracek, Y. F. Chaw, and V. A. V. Prasad, *J. Am. Chem. Soc.*, **99**, 3336 (1977).
(5) H. Wunderlich and D. Mootz, *Acta Crystallogr., Sect. B*, **30**, 935 (1974).
(6) T. E. Clark and R. R. Holmes, to be submitted for publication.
(7) R. O. Day, A. C. Sau, and R. R. Holmes, to be submitted for publication.
(8) R. S. Berry, *J. Chem. Phys.*, **32**, 933 (1960).
(9) R. R. Holmes and J. A. Deiters, *J. Am. Chem. Soc.*, **99**, 3318 (1977), and references cited therein.
(10) R. R. Holmes, *ACS Monogr.*, in press.
(11) R. K. Brown and R. R. Holmes, *J. Am. Chem. Soc.*, **99**, 3326 (1977).
(12) J. R. Devillers and R. R. Holmes, *J. Am. Chem. Soc.*, **99**, 3332 (1977).
(13) R. K. Brown and R. R. Holmes, *Inorg. Chem.*, **16**, 2294 (1977).
(14) J. A. Deiters, J. C. Gallucci, T. E. Clark, and R. R. Holmes, *J. Am. Chem. Soc.*, **99**, 5461 (1977).
(15) R. R. Holmes, *Acc. Chem. Res.*, **5**, 296 (1972).
(16) D. T. Cromer and J. T. Waber, *Acta Crystallogr.*, **18**, 104 (1965).
(17) R. F. Stewart, E. R. Davidson, and W. T. Simpson, *J. Chem. Phys.*, **42**, 3175 (1965).
(18) D. W. J. Cruickshank, "Crystallographic Computing," F. R. Ahmed, Ed., 1970, pp 187–197.
(19) (a) G. Germain, P. Main, and M. M. Woolfson, *Acta Crystallogr., Sect. A*, **27**, 368 (1971); (b) T. Debaerdemaeker and M. M. Woolfson, *ibid.*, **28**, 477 (1972).
(20) P. Coppens and W. C. Hamilton, *Acta Crystallogr., Sect. A*, **26**, 71 (1970).
(21) M. S. Lehmann and F. K. Larsen, *Acta Crystallogr., Sect. A*, 580 (1974).
(22) R. R. Holmes, *J. Am. Chem. Soc.*, **97**, 5379 (1975).
(23) R. J. Gillespie and R. S. Nyholm, *Q. Rev., Chem. Soc.*, **11**, 339 (1957); R. J. Gillespie, *Can. J. Chem.*, **38**, 818 (1960); *J. Chem. Educ.*, **40**, 295 (1963).
(24) R. R. Holmes, *J. Am. Chem. Soc.*, **96**, 4143 (1974).
(25) H. Wunderlich, personal communication.
(26) W. S. Sheldrick, personal communication.
(27) H. Wunderlich, *Acta Crystallogr., Sect. B*, **30** 939 (1974).
(28) H. Wunderlich, Third European Crystallographic Meeting, Zurich, Switzerland, Paper No. 054D, 1976.
(29) R. Sarma, F. Ramirez, and F. Maracek, *J. Org. Chem.*, **41**, 473 (1976).
(30) N. L. Allinger, M. T. Tribble, M. A. Miller, and D. H. Wertz, *J. Am. Chem. Soc.*, **93**, 1637 (1971).
(31) D. H. Wertz and N. L. Allinger, *Tetrahedron*, **30**, 1579 (1974).
(32) Reference 14, Table III.

Contribution from the Chemical Technology Division, Australian Atomic Energy Commission, Sydney, Australia

Crystal and Molecular Structure of Trimeric Bis(1,1,1,5,5,5-hexafluoropentane-2,4-dionato)dioxouranium(VI)

J. C. TAYLOR,* A. EKSTROM, and C. H. RANDALL

Received April 17, 1978

The deep red crystals of the title compound $[UO_2(hfa)_2]_3$ are monoclinic, space group $P2_1/c$, with a = 16.526 (11) Å, b = 15.470 (11) Å, c = 22.277 (15) Å, β = 103.00 (1)°, Z = 4, V = 5549 Å^3, and d_{calcd} = 2.457 g/cm^3. X-ray diffraction data were collected for 3239 independent reflections to 2θ = 36° on an automatic X-ray diffractometer with Mo Kα radiation, and the structure was refined to R = 0.095. The three uranium atoms in the asymmetric unit form an equilateral triangle with edges 4.2 Å in length and are bridged by half the uranyl oxygen atoms; the other uranyl oxygen atoms are terminal. The six hfa molecules in the asymmetric unit are bidentate and complete pentagonal-bipyramidal coordination about U(1), U(2), and U(3). The crystal is thus an assembly of $[UO_2(hfa)_2]_3$ trimeric molecules. The CF_3 groups are disordered. This compound is unique in uranyl structural chemistry, being the first example of a uranyl trimer.

Experimental Section

$[UO_2(hfa)_2]_3$ is extremely reactive and air sensitive. A sample was prepared by a method described elsewhere,[1] and crystals were grown in a quartz capillary by the technique of Edwards et al.[2] A suitable crystal was removed from its neighbors by vibration and wedged in a tapered section of the tube by careful tapping. The crystal was not in an orientation suitable for Weissenberg lineup, so the crystal data including cell dimensions were found directly on the automatic four-circle diffractometer. The symmetry was found to be monoclinic, space group $P2_1/c$, with a = 16.526 (11) Å, b = 15.470 (11) Å, c = 22.277 (15) Å, β = 103.00 (1)°, and V = 5549 Å^3. From the effective atomic volumes in other hfa complexes it was deduced that the unit cell held twelve $UO_2(hfa)_2$ units; this indicated a complex structure, probably trimeric. The unit cell contents were confirmed in the following structural analysis. The calculated density is 2.457 g cm^{-3}. Complete three-dimensional data were collected to 2θ = 36° with Mo Kα radiation (λ 0.7107 Å). A total of 3698 reciprocal lattice points were measured with a Si(Li) solid-state detector, and after averaging of equivalent reflections (which were measured for low-angle data only) 3239 reflections were available for the analysis. A standard reflection was measured every 20 reflections, and a 50% decline was observed in the standard over the period of the experiment (several weeks). The intensities were normalized to the standard reflection, corrected for absorption (μ = 54 cm^{-1} for Mo Kα, minimum and maximum transmission factors 13% and 24%), and reduced to $F(hkl)$ values.[3] The crystal faces were ±(100), ±(011), (0,1,−1), (1,0,−1), (2,−1,3), (−1,0,1), and (−1,−1,1), with distances from the crystal center of 250, 250, 157, 157, 330, 320, 300, 330, and 330 × 10^{-4} cm, respectively. The morphology was determined on the diffractometer with a calibrated microscope.

Structural Analysis

In the three-dimensional Patterson synthesis, 20 major peaks were observed as probable U–U vectors. This was consistent with the theoretical number of 9 (i–i)- and 12 (i–j)-type vectors for 3 independent uranium atoms U(1), U(2), and U(3) in $P2_1/c$. The (x, y, z) coordinates of U(1), U(2), and U(3) were deduced from the vectors by trial and error. The uranium atoms lay on the corners of an equilateral triangle of side 4.2 Å, confirming the trimeric nature of the molecule.

A structure factor calculation with the program LINUS,[4] with U(1),